Plant, Cell and Environment (2000) **23**, 279–289

Increased cytokinin levels in transgenic P_{SAG12}–*IPT* tobacco plants have large direct and indirect effects on leaf senescence, photosynthesis and N partitioning

W. JORDI,[1] A. SCHAPENDONK,[1] E. DAVELAAR,[1] G. M. STOOPEN,[1] C. S. POT,[1] R. DE VISSER,[1] J. A. VAN RHIJN,[2] S. GAN[3] & R. M. AMASINO[4]

[1]Research Institute for Agrobiology and Soil Fertility (AB), PO Box 14, 6700 AA Wageningen, The Netherlands, [2]RIKILT, Post Box 230, 6700 AE Wageningen, The Netherlands, [3]Department of Agronomy and Tobacco and Health Research Institute, University of Kentucky, Lexington, KY 40546, USA, and [4]Department of Biochemistry, 433 Babcock Dr, University of Wisconsin, Madison, WI 53706-1544, USA

ABSTRACT

We studied the impact of delayed leaf senescence on the functioning of plants growing under conditions of nitrogen remobilization. Interactions between cytokinin metabolism, Rubisco and protein levels, photosynthesis and plant nitrogen partitioning were studied in transgenic tobacco (*Nicotiana tabacum* L.) plants showing delayed leaf senescence through a novel type of enhanced cytokinin synthesis, i.e. targeted to senescing leaves and negatively auto-regulated (P_{SAG12}–*IPT*), thus preventing developmental abnormalities. Plants were grown with growth-limiting nitrogen supply. Compared to the wild-type, endogenous levels of free zeatin (Z)- and Z riboside (ZR)-type cytokinins were increased up to 15-fold (total ZR up to 100-fold) in senescing leaves, and twofold in younger leaves of P_{SAG12}–*IPT*. In these plants, the senescence-associated declines in N, protein and Rubisco levels and photosynthesis rates were delayed. Senescing leaves accumulated more (^{15}N-labelled) N than younger leaves, associated with reduced shoot N accumulation (–60%) and a partially inverted canopy N profile in P_{SAG12}–*IPT* plants. While root N accumulation was not affected, N translocation to non-senescing leaves was progressively reduced. We discuss potential consequences of these modified sink–source relations, associated with delayed leaf senescence, for plant productivity and the efficiency of utilization of light and minerals.

Key-words: canopy N profile; chlorophyll; cytokinins; isopentenyl transferase; N-15; photosynthesis; Rubisco; remobilization; senescence-associated gene; sink activity; transgenic plants.

INTRODUCTION

Leaf senescence is not simply a degenerative process but a type of programmed cell death that plays an important role in the recycling of nutrients from old, non-functional leaves to young productive leaves and developing seeds. In the field situation, leaf senescence contributes to efficient utilization of minerals and light energy (Pons *et al*. 1989; Wright & Hammer 1994; Livingston *et al*. 1998), through the remobilization of nutrients to younger leaves (Smart 1994; Schnyder & De Visser 1999). The process is biochemically characterized by a loss of chlorophyll (yellowing), protein, lipids and RNA (for reviews see Smart 1994; Gan & Amasino 1997). Leaf senescence is under strict nuclear control. While most genes are inactivated during leaf senescence, distinct sets of genes are activated (referred to as SAGs, senescence-associated genes; Gan & Amasino 1997). The newly expressed genes include regulatory genes involved in switching on the 'senescence programme', and genes encoding proteins that break down pigments, RNA, lipids or proteins. Furthermore, genes which play a role in the recycling of nutrients, such as glutamine synthetase, are induced in senescing leaves.

Various internal and external stimuli may induce the leaf senescence programme. The external stimuli include changes in light flux and quality, temperature, drought, mineral deficiency and pathogen attack. These factors interact with each other and with internal factors such as carbohydrate level (e.g. Guitman, Arnozis & Barneix 1991; Jordi *et al*. 1994; Wingler *et al*. 1998), age, reproduction and phytohormones or plant growth regulators (PGRs) in triggering leaf senescence (Thimann 1980; Goldthwaite 1988). PGRs can promote or delay leaf senescence (for reviews see Smart 1994; Gan & Amasino 1997). Ethylene, methyljasmonate and abscisic acid are thought to enhance or trigger senescence, whereas cytokinins, gibberellins and auxins have been reported to delay senescence. Until recently, these roles of PGRs in leaf senescence were deduced from correlations between senescence and exo- or endogenous PGR levels.

Recently, many genes which direct the biosynthesis and perception of PGRs have been cloned, enabling the manipulation of PGR levels and action in transgenic plants. Such experiments directly demonstrated retarded leaf

Correspondence: Ries de Visser. Fax: +31 317 423110; E-mail: a.j.c.devisser@ab.wag-ur nl

© 2000 Blackwell Science Ltd

senescence in tomato plants which have low levels of ethylene biosynthesis (John *et al*. 1995) or in *Arabidopsis* with disrupted ethylene perception (Grbic & Bleecker 1995). Transgenic plants expressing a bacterial gene encoding isopentenyl transferase (IPT), a key enzyme in cytokinin biosynthesis, exhibit enhanced cytokinin production and delayed leaf senescence (Gan & Amasino 1995, 1997; Wang *et al*. 1997). Cytokinins are regulators of a variety of developmental processes in addition to leaf senescence, such as rooting and apical dominance (McKenzie *et al*. 1998), cell division and assimilate import and partitioning (Brenner & Cheikh 1995) and vascular tissue differentiation (Aloni 1995). To avoid direct interference with these other aspects of normal plant development, a highly senescence-specific *SAG12* promoter has been used to target cytokinin biosynthesis to the senescing tissues in transgenic P_{SAG12}–*IPT* tobacco plants (Gan & Amasino 1995). The inhibition of leaf senescence also attenuates the senescence-specific promoter (Gan & Amasino 1997), preventing accumulation of cytokinins to levels that interfere with normal plant development and gene expression (Medford *et al*. 1989; Schmülling, Schäfer & Romanov 1997; Wang *et al*. 1997; McKenzie *et al*. 1998). This autoregulatory loop results in novel plants with strongly delayed leaf senescence without further phenotypic developmental abnormalities (Gan & Amasino 1997). In a recent study with this plant material, Wingler *et al*. (1998) demonstrated a delayed decline of photosynthetic activity of old leaves and a co-regulating role of cytokinins, light and sugars in the senescence-related decline of various photosynthetic enzymes.

In this paper, we studied the impact of delayed leaf senescence on the functioning of plants growing under conditions of N remobilization, using P_{SAG12}–*IPT* tobacco plants with autoregulated synthesis of cytokinins in senescing leaves. We determined endogenous cytokinin levels of leaves and studied the consequences of modified cytokinin metabolism and delayed leaf senescence for photosynthesis and protein levels of leaves and N partitioning of the plant.

MATERIALS AND METHODS

Plant material

In two experiments, cytokinins, photosynthesis and chemical composition were analysed. In the first experiment, the seeds were sown on 18 September 1995 (total of 56 plants; Wageningen). In the second experiment, the seeds were sown on 28 September 1996 (total of 80 plants; Wageningen). The phenotype of the plants was identical in both experiments and comparable to the previously reported phenotype (Gan & Amasino 1995). These experiments gave similar results; in this paper we report on the second experiment. Seeds of wild-type (WT) and transgenic P_{SAG12}–*IPT* (SAG–IPT; see Introduction) tobacco (*Nicotiana tabacum* L. cv. Wisconsin 38) were germinated in compost. For detailed information on the P_{SAG12}–*IPT* construct, see Gan & Amasino (1995, 1997). Plants hemizygous and homozygous for P_{SAG12}–*IPT* were grown and analysed for cytokinins. Two weeks after sowing, plants were transferred to 110 mL pots with Klasmann substrate no. 4 containing 210 mg L^{-1} N (as NH_4NO_3), 240 mg L^{-1} P_2O_5, 275 mg L^{-1} K_2O and 115 mg L^{-1} MgO, pH 5·5–6·0. The plants were grown at a relative humidity of 75%, day/night temperatures in the greenhouse were 21°C/18 °C. Supplementary light was provided for 16 h at a photosynthetic photon flux density (PPFD) of 140 μmol m^{-2} s^{-1} at the top of the plants. The total light intensity averaged about 400 μmol m^{-2} s^{-1}. Five weeks after sowing, the plants (28 WT, 28 P_{SAG12}–*IPT* hemizygous and 24 P_{SAG12}–*IPT* homozygous) were transferred to 2·5 L containers with Klasmann substrate no. 4 arranged according to a randomized block design in the greenhouse. After 6 weeks, each plant received 100 mL of a Steiner solution (Steiner 1984). Afterwards only water was supplied to the plants. Ten weeks after sowing, photosynthesis measurements were started with two groups of four plants (WT and P_{SAG12}–*IPT* hemizygous) and analysed for a period of 3–4 weeks. Eleven weeks after sowing, leaf material was collected for biochemical analyses. For each of the three types of plants (WT, hemi- and homozygous P_{SAG12}–*IPT*), four groups of six plants each were analysed and leaf material of different leaf number was collected and frozen in liquid N_2. Five groups of leaves were distinguished, numbered in order of appearance as 3–4, 7–10, 12–15, 16–18 and 19–26. After 11 weeks, plants had 26 (SD 1·5) leaves on the main stem. Photosynthesis of five leaves was measured in four replicates as a function of developmental stage of the plant (at 11 and 15 weeks after sowing). The leaves selected for this purpose were numbers 3, 6, 9, 12, and 15 (the youngest leaf of 11-week-old plants with sufficient area for gas-exchange measurements).

Chlorophyll content and light absorption

Chlorophyll $a + b$ contents of a number of leaves were determined spectrophotometrically after extraction with dimethylformamide (Inskeep & Bloom 1985) and the results were related to the red light (640 nm) transmission readings of a hand-held automated chlorophyll meter, SPAD-502 (Minolta, Japan). Absorption of light between 400 and 700 nm was measured with a LICOR model LI-1800 radiospectrophotometer (LICOR Inc., Lincoln, Nebraska, USA) and expressed as fraction of maximum absorption.

Gas exchange

Leaf photosynthesis and transpiration rates were measured using four cuvettes of the 'open system' type, running in parallel. Air velocity over the leaf was 1·5 m s^{-1}. The boundary layer conductance to H_2O was 0·7 mol m^{-2} s^{-1}. Photosynthesis and transpiration rates were calculated from the flow rates and the concentrations of CO_2 and water vapour in the in-going and out-going air, according to von Caemmerer & Farquhar (1981). Photosynthesis was measured at six different irradiances up to 1·5 mmol m^{-2} s^{-1}

(PPFD). Maximum photosynthetic capacity (A_{max}) was determined in saturating CO_2 (900 μL L^{-1}). A_{max} was derived from apparent steady-state rates at the highest light intensity. Leaves were acclimatized to the light conditions for half an hour prior to the measurements.

Soluble proteins and Rubisco

Soluble proteins and Rubisco were extracted and determined as described by Jordi *et al*. (1996), starting with grinding leaves (approximately 1 g fresh weight) in a pre-cooled mortar under liquid nitrogen. Protein patterns were visualized by applying 5 μL of the protein extracts on a 12% SDS–polyacrylamide gel and staining with Coomassie brilliant blue (R250). Rubisco was quantified by densitometry of the protein bands using bovine serum albumin as a standard.

Cytokinins

Purification, separation and quantification of cytokinins were performed as described by Vonk, Davelaar & Ribôt (1986), with minor modifications. Samples were powdered in liquid N_2 and extracted in boiling ethanol (10 min). After centrifugation, pellets were re-extracted twice in ethanol 80%. Ethanol was removed by evaporation under reduced pressure and the aqueous residues were taken up in water. After freezing and thawing, precipitated material was removed by centrifugation. For the separation of free and bound cytokinins, samples were partitioned (pH 8·2) against water-saturated butan-1-ol (I). The water layer was treated with acid phosphatase (pH 6) and re-extracted with water-saturated butan-1-ol (II). Butanol layers I and II represent free and bound cytokinins, respectively. Butanol layers were evaporated to dryness. Purification of samples was performed by a combination of anionic exchange and reverse-phase C18 column chromatography. Subsequently, zeatin (Z), Z riboside (ZR), isopentenyl adenine (IPA) and IPA riboside (IPAR) were separated by HPLC and cytokinin quantification was performed by an enzyme immunoassay (EIA). For quantification of cytokinins as IPAR and ZR equivalents, total samples were treated with acid phosphatase (pH 6·0). Samples were treated as described above without the HPLC separation. [^{3}H]ZR was added to determine the recovery during the purification procedure. Total recovery after the procedure was 84%. The ZR and IPAR antibodies exhibit cross-reactivities of 40·5 and 40% to Z and isopentenyladenine, respectively. Cross-reactivity of ZR and IPAR antibodies to cytokinins of IPA- and Z-type, respectively, was typically less than 0·5%. The ZR antibodies exhibited a limited but significant cross-reactivity of 0·3% to dihydrozeatin (Vonk *et al*. 1986). The combined contents of Z, ZR and bound ZR are referred to as ZR equivalents.

For quantification and identification of cytokinins in the oldest leaves of selected WT and transgenic plants by liquid chromatography-tandem mass spectrometry (LC-tandem MS) (Redig *et al*. 1997; van Rhijn *et al*. 2000), phosphatase-treated samples purified by the combination of anionic exchange and reverse-phase C18 column chromatography were further purified by immunoaffinity column chromatography (IAC). $^2H_5$-Z, $^2H_5$-Z-9-G, $^2H_3$-dihydrozeatin riboside (DHZR), $^2H_6$-IPA, $^2H_6$-IPAR and $^2H_6$-IPA-9-G (10 ng of each) were added as internal tracers. Samples were dissolved in PBS buffer (pH 7·2) and passed through a combination of a non-immune column (1 mL) and an immunoaffinity column (0·5 mL). Non-immune columns were prepared by coupling rabbit γ-globulins to CNBr-activated Sepharose 4B. Immunoaffinity columns were prepared by coupling polyclonal antibodies against ZR, IPAR and DHZR to CNBr-activated Sepharose 4B. They had a binding capacity of more than 1000 pmol of each cytokinin per 0·5 mL gel. After washing with 5 mL PBS buffer (pH 7·2) and 10 mL water (pH 7·0), the immunoaffinity columns were eluted with 5 mL of ice-cold methanol. Eluates were evaporated until dryness. The dry sample extracts resulting from the IAC procedure were dissolved in 100 μL of demineralized water. The extract was transferred to the insert of a sample vial and a 20 μL aliquot was used for analysis. Standard solutions containing 2·5, 5·0, 10, 20 and 50×10^{-8} mol L^{-1} of each of the cytokinins were used for calibration. The internal standards were present at the same level as in the sample extracts. For all cytokinins, a linear calibration curve was obtained. The limit of detection was estimated at 100 fmol g^{-1} FW for the N-9-glucosides and 50 fmol g^{-1} FW for all other compounds. Separation of the cytokinins was achieved on a Phenomenex (Torrance, California, USA) LUNA C8, 5 μm, $150 \times 1{\cdot}0$ mm column. The column was pumped at a flow rate of 60 μL min^{-1} using a gradient HPLC system comprised of a Gyncotek 300 and 480 pump (Germering, Germany). A linear gradient from 10–80% methanol in 10 mM ammonium acetate was applied. Aliquots of 20 μL were injected at 45 min intervals using a Gilson 231-401 autosampler. The column was connected directly to a Finnigan MAT (San Jose, California, USA) electrospray ion source mounted on a Finnigan MAT TSQ 700 mass spectrometer. The electrospray source was operated at standard settings, i.e. sheath gas pressure adjusted to 0·5 MPa, the spray voltage set at 5 kV and the heated capillary at 225 °C. Tandem mass spectra were recorded in daughter mode using argon as the collision gas adjusted to a pressure of 2 mTorr. The collision offset was adjusted to obtain optimum fragmentation of the parent ion towards the selected daughter ion. For all individual compounds, MS and tandem MS spectra were recorded by continuous infusion of a 1 ng μL^{-1} solution in 50/50 methanol/10 mM ammonium acetate at a flow rate of 5 μL min^{-1}. Data acquisition for quantitative analysis was performed in single reaction monitoring (SRM) mode, recording the loss of the riboside or glucoside moiety for the glycosylated compounds, while for the aglycones the loss of the pentanol moiety was monitored. For the isotopically labelled internal standards, analogous fragmentations were monitored. A more detailed description of the analytical procedure is presented elsewhere (van Rhijn *et al*. 2000).

Steady-state ^{15}N labelling and N partitioning

The current partitioning of nitrogen was examined in two experiments with N-starved plants showing senescence of old leaves by steady-state labelling with ^{15}N-nitrate (Chemotrade mbH, Leipzig, Germany) according to procedures described by Deléens *et al*. (1994) and De Visser, Vianden & Schnyder (1997). We present the results of the second of two similar experiments. Plants were grown in aerated nutrient solution (Steiner 1984) to enable sampling of root biomass and control of (^{15}N-)nitrate supply to the plants. Other growth conditions were similar to those described above; however, growth period was December 1997–February 1998, and supplementary light was provided for 16 h at a PPFD of 60 μmol m^{-2} s^{-1} to a maximum of 380 μmol m^{-2} s^{-1} at the top of the plants. Four weeks after sowing, the plants (40 WT and 40 P_{SAG12}–*IPT* hemizygous) were transferred to 10 L containers (avoiding mutual shading), connected in parallel to a continuous flow system (total volume 300 L) with Steiner nutrient solution (Steiner 1984; Schapendonk, Spitters & de Vos 1990), and arranged according to a randomized block design in the greenhouse. Six weeks after sowing, the plants received N-free Steiner solution. Steady-state labelling with ^{15}N-nitrate (0·1 mM; 10 atom% ^{15}N; cf De Visser *et al*. 1997) was started 12 weeks after sowing, with five WT and five P_{SAG12}–*IPT* hemizygous plants, and continued for a period of 24 h. Subsequently, plants were dissected and plant tissue samples were oven-dried at 80 °C. From total N content and ^{15}N abundance (atom% ^{15}N), the amounts of N originating from reserves and current assimilates were calculated for the various plant parts (De Visser *et al*. 1997). Current partitioning of (labelled) N was expressed by two parameters, relative specific allocation of N (RSA_N, g N (labelled) g^{-1} N (total) per day; a measure of the current sink activity of a specific plant organ for N) and current relative partitioning of N between organs within the plant (%P_N (g N (labelled) in an organ g^{-1} N (labelled) in the plant) × 100%; Deléens *et al*. 1994).

RESULTS

The transgenic P_{SAG12}–*IPT* (SAG–IPT) tobacco plants, expressing a bacterial gene encoding IPT under control of the senescence-specific *SAG12* promoter, retained chlorophyll and turgor in the older leaves in contrast to the WT plants (Fig. 1), until the stage of flowering, as previously reported by Gan & Amasino (1995) and Wingler *et al*. (1998). We have observed no further phenotypic abnormalities in the SAG–IPT plants apart from 5 and 10% reductions, relative to the WT, in average plant height in the hemizygous and homozygous SAG–IPT plants, respectively.

Chlorophyll and protein contents

The contents of chlorophyll, soluble protein and Rubisco dropped dramatically from young to old leaves of the WT, while in old leaves of the SAG–IPT plants chlorophyll was maintained at 100% (Fig. 2a), soluble protein at 30% (Fig. 2b) and Rubisco at 15% (Fig. 2c; $P < 0{\cdot}01$) of the respective levels in young leaves. However, the contents of these components in the youngest leaves of SAG–IPT were lower ($P < 0{\cdot}05$) than those in the WT plants. The leaf protein content of the oldest SAG–IPT leaves was decreased by 65% relative to the youngest leaves (Fig. 2b), significantly less than the corresponding decrease in Rubisco content (85%; $P < 0{\cdot}05$; Fig. 2c).

Figure 1. Typical phenotypes of wild-type (WT; left) and hemizygous SAG–IPT transgenic plants (P_{SAG12}–*IPT*; right) of tobacco 11 weeks after sowing.

Photosynthesis and leaf PPFD absorption

Hemizygous SAG–IPT plants were compared with WT because of their greater similarity in plant height as compared to WT. In week 11, the fractions of PPFD absorbed by old leaves and young leaves of hemizygous SAG–IPT plants were about 0·8 (Fig. 3a), and significantly higher than the fractions absorbed by old leaves (numbers 3–6) of WT which showed values of 0·5 or less ($P < 0{\cdot}01$). These leaves were wilted in week 15. By contrast, the older SAG–IPT leaves maintained turgor and a higher PPFD absorption than WT (leaf numbers 3, 6 and 9; Fig. 3b). In addition, for all leaves except the youngest, the decline of absorption between weeks 11 and 15 was slower in SAG–IPT plants (cf Fig. 3a,b).

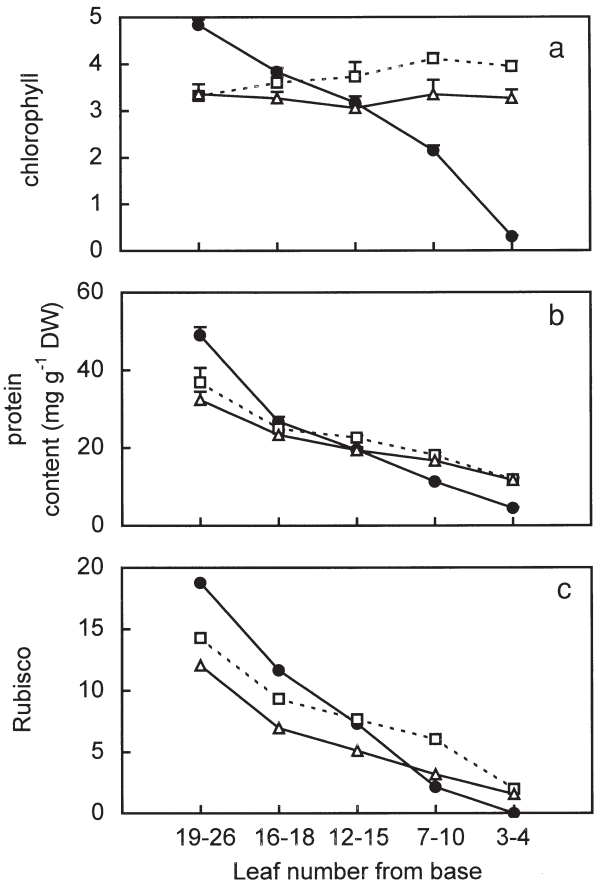

Figure 2. Contents of chlorophyll $a + b$ (a), total soluble protein (b) and Rubisco (c) of leaves from different positions on the main stem of 11-week-old plants of wild-type (WT; closed circles) and homozygous (open squares) and hemizygous SAG–IPT (open triangles; P_{SAG12}–*IPT*) tobacco. Five leaf age groups were distinguished, leaves numbered in order of appearance: leaves 3–4 (oldest live leaves), 7–10, 12–15, 16–18 and 19–26 (youngest leaves). Vertical bars denote SE, $n = 4$. If no bar is visible, SE is smaller than symbol size.

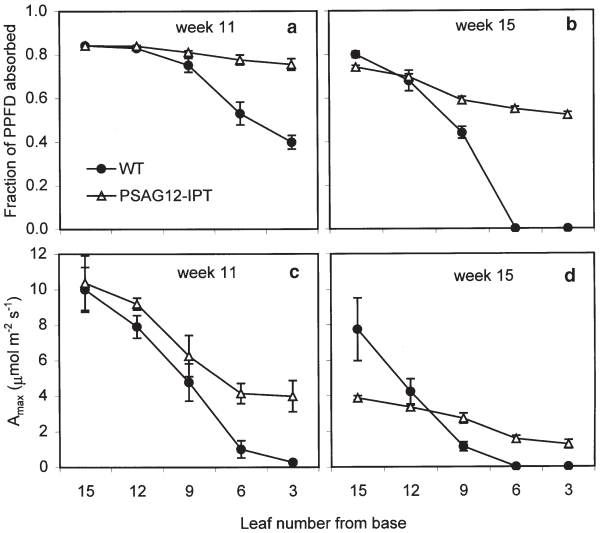

Figure 3. PPFD absorption (a,b) and A_{max} (c,d) of leaves of wild-type (WT, closed circles) and hemizygous SAG–IPT (open triangles; P_{SAG12}–*IPT*) tobacco as a function of leaf number and time (a and b, 11 and 15 weeks after sowing, respectively). Leaves were numbered in order of appearance; in week 15, oldest WT leaves were desiccated. Bars indicate 2 × SE; $n = 4$.

In week 11, the A_{max} values of all SAG–IPT leaves below leaf no. 15 were higher than those of the WT (Fig. 3c; $P < 0{\cdot}01$ for leaves 3 and 6). We found no effect of P_{SAG12}–*IPT* on the initial slope of the light response curves, suggesting that electron transport was not involved in the effect on photosynthetic performance. The A_{max} of the youngest WT leaves was about 30 times higher than the A_{max} of leaf 3. The oldest leaves of the (hemizygous) SAG–IPT plants retained a low but significant rate of photosynthesis during the entire period of the experiment. Overall, these results for the hemizygous SAG–IPT and WT in week 11 closely match the data on delayed decline of leaf photosynthesis rates presented by Wingler *et al.* (1998).

During N-limited growth between weeks 11 and 15, A_{max} declined by 80–100% in old leaves and by 23% in young leaves of WT, and, in contrast, by about 63% in all leaves of hemizygous SAG–IPT. Thus, in terms of A_{max}, SAG–IPT showed a lower rate of senescence (– 63% versus – 90% in WT) in old leaves (as expected) but a higher rate (– 63% versus – 23% in WT) in young leaves (Fig. 3c,d). On a Rubisco basis, however, A_{max} showed negligible differences between SAG–IPT and WT (results not shown).

Cytokinins

The transgenic P_{SAG12}–*IPT* plants were engineered to target cytokinin biosynthesis to senescent leaves (Gan & Amasino 1995). We have identified various cytokinins in the leaves of the present WT and transgenic plants, using both EIA (Vonk *et al.* 1986; Table 1) and LC-tandem MS (Redig *et al.* 1997; van Rhijn *et al.* 2000; Table 2). We have analysed the Z and IPA types of cytokinins in leaves of different ages in WT and SAG–IPT plants. The levels of IPA -equivalents in leaves of both homo- and hemizygous SAG–IPT plants were always between 10 and 20 pmol g^{-1} DW (or 2 and 4 pmol g^{-1} FW). No significant increase in the levels of IPAR equivalents in older leaves was observed (data not shown), in agreement with previous studies on transgenic

Table 1. Levels (pmol g^{-1} DW) of zeatin (Z), free zeatin riboside (ZR) and bound ZR, in the oldest leaves of wild-type and hemi- and homozygous P_{SAG12}–*IPT* (SAG–IPT) tobacco plants; $n = 4$; numbers in parentheses indicate SE

	Z	ZR	Bound ZR
Wild-type	2·0 (0·3)	2·1 (0·2)	0·3 (0·1)
Homozygous SAG–IPT	29·8 (2·7)	24·3 (2·6)	364 (42)
Hemizygous SAG–IPT	21·5 (1·3)	13·6 (1·1)	145 (21)

Table 2. The content (pmol g^{-1} DW) of a number of selected cytokinins in acid phosphatase treated samples (i.e. free + bound forms) of oldest (senescing) leaves of wild-type and SAG–IPT tobacco plants, determined and identified by LC-tandem MS analysis; for comparison, results of EIA analyses of the same samples are shown in parentheses; $n = 1$.

	IPA	IPAR	N9G-Z	N9G-DHZ	Z	DHZ	ZR	DHZR
Wild-type	0·25	12·8	< 0·5	< 0·5	0·2 (1·5)	< 0·2	< 0·2 (1·9)	0·53
Homozygous SAG–IPT	1·16	8·8	< 0·5	< 0·5	30·0 (21·4)	0·95	182 (203)	0·84
Hemizygous SAG–IPT	0·87	7·0	< 0·5	< 0·5	24·7 (21·9)	1·42	309 (234)	1·26

N9*G*-DHZ, dihydrozeatin-9-glucoside; N9G-Z, zeatin-9-glucoside

plants expressing the *IPT* gene which indicated that the IPA-type cytokinins were rapidly converted into the Z-type cytokinins (Smart *et al*. 1991; Zhang *et al*. 1995). For this reason, IPA-type cytokinins will not be further described or discussed. Figure 4 demonstrates the dramatic increase in zeatin riboside (ZR) equivalents in the oldest leaves in both the SAG–IPT homo- and hemizygous plants as compared to WT plants. In the inset of Fig. 4, with exploded scale, it is shown that in the small, youngest leaves at the top of the SAG–IPT plants ZR equivalents were also slightly but significantly increased as compared to corresponding WT leaves ($P < 0·01$). In the mature and young leaves (numbers 10–21), the levels of ZR equivalents in homozygous SAG–IPT were significantly higher than in the hemizygous plants ($P < 0·05$; Fig. 4). Cytokinins were separated into Z free base, nucleoside and nucleotide (Z free and bound forms as described above; Table 1). No bound Z was detected after HPLC separation of the acid phosphatase-treated water phase.

The increase in Z-type cytokinins in old leaves of SAG–IPT plants is composed of free Z and ZR. In addition to increases in these presumed biologically active cytokinins, a strong increase in bound ZR is observed in the old leaves of SAG–IPT plants as compared to the WT plants (Table 1). The content of a number of selected cytokinins in phosphatase-treated samples of oldest leaves of three genotypes was determined using LC-tandem MS analysis (Table 2). The results essentially confirmed the EIA measurements (in brackets) with the exception of the Z–ZR equivalents in the WT plants. The latter result is probably due to interfering compounds in the EIA assay in the old senescing leaves of WT plants.

N partitioning

N distribution and partitioning were studied in 12-week-old WT and hemizygous SAG–IPT plants. Differences in leaf dry weight between WT and SAG–IPT were small (except for leaves 7–9, which were partially wilted in WT; Fig. 5a). Relative to the WT, the N concentration (g/g) in old leaves (numbers 3–6) of SAG–IPT was 20% higher, while in the young leaves (numbers 16–21) and shoot apex it was 25%

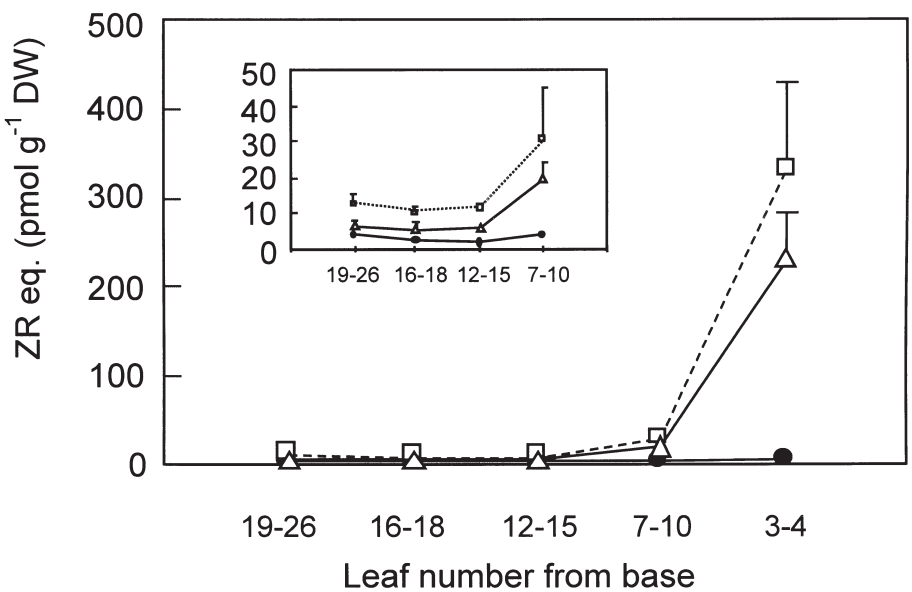

Figure 4. Zeatin riboside (ZR) equivalents in leaves at different positions on the main stem of 11-week-old plants of wild-type (WT; closed circles) and homozygous (open squares) and hemizygous SAG–IPT (open triangles; P_{SAG12}-*IPT*) tobacco. ZR equivalents (free + bound) are plotted on two different scales in the main frame and inset. Bars indicate 2 × SE; $n = 4$. For further information, see the legend to Fig. 2.

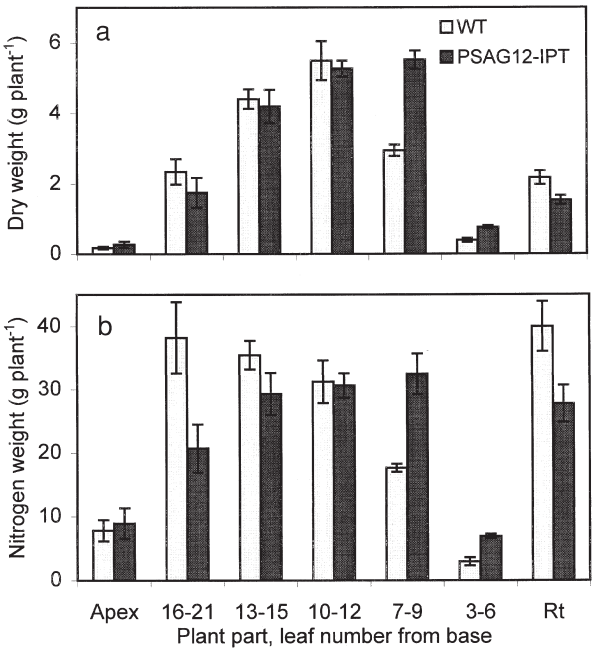

Figure 5. Distribution of dry matter (a) and total nitrogen (b) over plant parts, including the various leaf age groups, shoot apex and roots of wild-type (open columns) and hemizygous SAG–IPT (filled columns; P_{SAG12}–*IPT*) tobacco; bars indicate 2 × SE; $n = 4$.

lower (results not shown; $P < 0{\cdot}05$). N weight (Fig. 5b; g/plant) was higher in old leaves (numbers 3–6 and 7–9) and lower in the youngest leaves (numbers 16–21) of SAG–IPT plants ($P < 0{\cdot}02$) as compared to WT. This effect can be summarized as 'inverted canopy N profile' in SAG–IPT. It indicates differences in N partitioning between WT and hemizygous SAG–IPT which may increase with time. Indeed, this was clearly shown by steady-state ^{15}N-labelling of plants for 1 day: SAG–IPT plants showed a higher accumulation rate of currently absorbed, ^{15}N-labelled N (RSA_N) in senescing leaves 7–9, but a lower N accumulation rate in the younger leaves as compared to WT ($P < 0{\cdot}01$; Fig. 6a). Moreover, not only was current (^{15}N-labelled) N translocation to young leaves decreased in hemizygous SAG–IPT, but the current N accumulation rate of the whole plant was also decreased in the SAG–IPT plants (RSA_N lower than WT in most leaves; Fig. 6a) by approximately 60%, while the N accumulation rate of the roots was similar to that of the WT (Fig. 6a). The current partitioning of (^{15}N-labelled) N between plant parts ($\%P_N$; Fig. 6b) closely resembled the distribution of total N (Fig. 5b), although the differences between SAG–IPT and WT in $\%P_N$ were more pronounced, especially in leaf numbers 7–9, 13–15 and 16–21 ($P < 0{\cdot}01$). Moreover, roots showed a relatively high accumulation rate of currently absorbed N, especially in the SAG–IPT plants (Fig. 6b; $P < 0{\cdot}01$).

Increased cytokinin levels in a plant organ are generally associated with delayed senescence and increased sink activity, in terms of specific accumulation rate of assimilates (Leopold & Kawase 1964; Brenner & Cheikh 1995; Wingler *et al.* 1998). Indeed this was found in the older leaves of the present plant material, comparing WT and SAG–IPT. In young SAG–IPT leaves, on the other hand, sink activity for N was decreased relative to the WT, even though ZR equivalents were similar or higher (Fig. 7). In conclusion, our data demonstrate that in SAG–IPT plants sink activities for N in the various leaf age classes are very similar and more homogeneous than in the WT, leading to a shift in N distribution from young to old leaves ('inverted canopy N profile').

DISCUSSION

Effects of P_{SAG12}–*IPT* on nitrogenous leaf components and photosynthesis

The increase in cytokinin levels in the oldest leaves of P_{SAG12}–*IPT* (SAG–IPT) plants has profound direct effects on leaf senescence (cf Fig. 8). The most obvious features are a complete retention of chlorophyll and an increased photosynthesis rate and life span of the older SAG–IPT leaves. In this respect, we have confirmed the conclusions and model presented by Wingler *et al.* (1998). A_{max} and PPFD absorption generally decreased with leaf age between weeks 11 and 15 (Fig. 3). However, while this decrease was strongest in old leaves of the WT, such an effect of leaf age

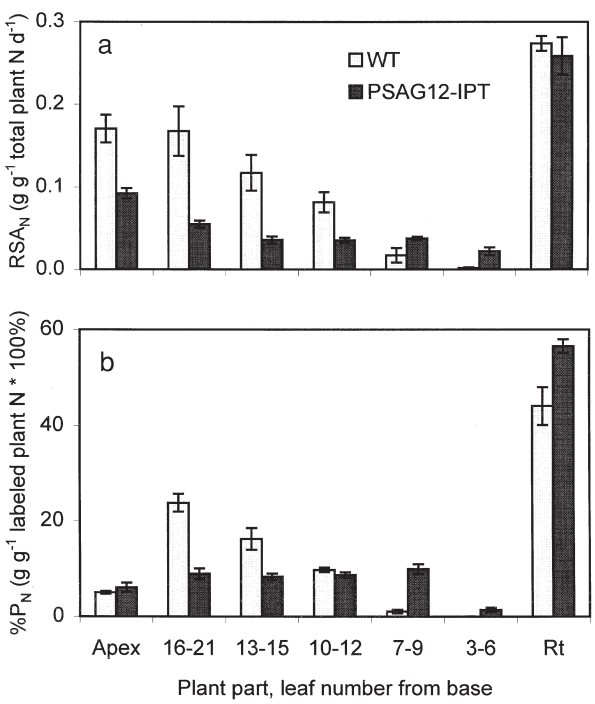

Figure 6. Current N sink activity of various leaf age groups (RSA_N; a) and current plant N partitioning over all plant parts including the various leaf age groups, shoot apex and roots ($\%P_N$; b) of wild-type (open columns) and hemizygous SAG–IPT (filled columns; P_{SAG12}–*IPT*) tobacco during ^{15}N-labelling; bars indicate 2 × SE; $n = 4$.

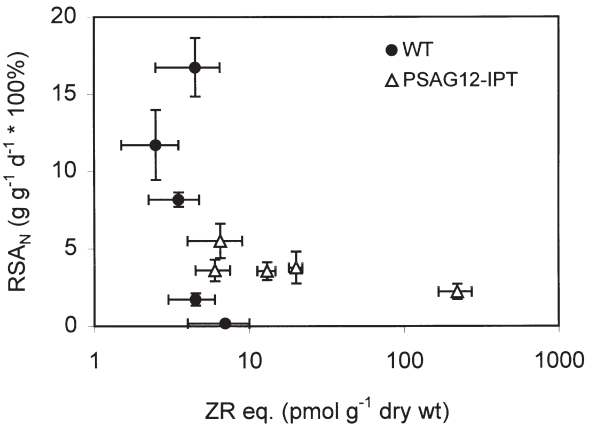

Figure 7. Relationship between current N sink activity (RSA_N), as determined by steady-state ^{15}N-labelling, and leaf cytokinin (ZR equivalents) levels of the various leaf age groups in wild-type (closed circles) and hemizygous SAG–IPT (open triangles; P_{SAG12}-*IPT*) tobacco; bars indicate 2 × SE; $n = 4$.

was not evident in SAG–IPT leaves. In fully unfolded young leaves (leaf 15) of SAG–IPT, we found a dramatic decline of A_{max} between weeks 11 and 15, as compared to young WT leaves. Expression of *IPT* in older leaves causes maintenance of chlorophyll content and PPFD absorption but is less effective in delaying other aspects of senescence such as loss of soluble protein, and still less effective in maintaining Rubisco and photosynthesis levels. Possibly, higher cytokinin levels or additional triggers (e.g. light or N; see Wingler *et al*. 1998 and Fig. 8) delay the latter senescence processes. The distinct effect of *IPT* expression on various senescence parameters may be caused by the growth-limiting N supply chosen here to induce leaf senescence (Fig. 8). Nutrients may be exported to younger parts of the plant before the promoter is activated or remobilization may not be completely inhibited by the action of SAG–IPT. Comparing leaves of similar age, hemizygous SAG–IPT leaves often have lower photosynthesis rates per unit absorbed light than the WT leaves, mainly in old leaves in week 11 and in young leaves in week 15 (cf Fig. 3a,b versus 3c,d, respectively). This suggests increased dissipation of excess light energy in SAG–IPT leaves (cf Niyogi 1999). Apparently, not all processes required for a high light-use efficiency are maintained through the senescence-specific expression of *IPT,* when N is limiting growth.

A comparison of the effects of P_{SAG12}–*IPT* on young and old leaves reveals striking differences. In contrast to the (expected) retention of chlorophyll, Rubisco and protein in the older leaves of the SAG–IPT plants, their younger leaves had a lower content of chlorophyll, protein and Rubisco than corresponding young leaves of WT plants. We show that this is caused by inhibition of remobilization of nutrients from older leaves to younger leaves of the SAG–IPT plants (see section on N partitioning below). One of the consequences of the differential effects of P_{SAG12}–*IPT* on the photosynthetic characteristics of young and old leaves may be reduced productivity. Because the young, upper leaves of plants are most important for interception of light under field conditions (Pons *et al*. 1989; Wright & Hammer 1994), the negative effect on the photosynthetic components of the upper leaves of the SAG–IPT plants may seriously limit potential increases in biomass of these plants under limited N nutrition.

The relationships between A_{max}, irradiance and leaf N and Rubisco levels were close to theoretical and experimental estimates (Hikosaka & Terashima 1995). In particular, the relationship between A_{max} and Rubisco level was close ($r^2 = 0{\cdot}98$), and similar for WT and hemizygous SAG–IPT. We therefore conclude that the rate of senescence-associated decline of Rubisco activity in the SAG–IPT leaves is similar to the decline in the WT leaves. Taken together, the data show that increased cytokinin levels in old leaves have differential effects on the various components of the photosynthetic system in old leaves, and indirect effects on the functioning of young leaves via changes in N partitioning between plant parts (see below).

Effects of P_{SAG12}–*IPT* on levels of cytokinins

In contrast to transgenic tobacco lines over-expressing IPT under the control of other promoters (e.g. Wang *et al*. 1997; McKenzie *et al*. 1998), hemizygous *SAG–IPT* plants clearly showed autoregulatory cytokinin synthesis, resulting in tissue concentrations of Z(R) which were up to one (McKenzie *et al*. 1998) or two (Wang *et al*. 1997) orders of magnitude lower than in these other promoter–IPT systems (cf Tables 1 and 2, Fig. 4). Maximum levels ranged from 20 (hemizygous SAG–IPT) to 30 pmol g^{-1} FW (homozygotes). Moreover, cytokinin biosynthesis in SAG–IPT plants was mainly targeted to senescing leaves (Fig. 4), which prevented developmental changes such as the breaking of

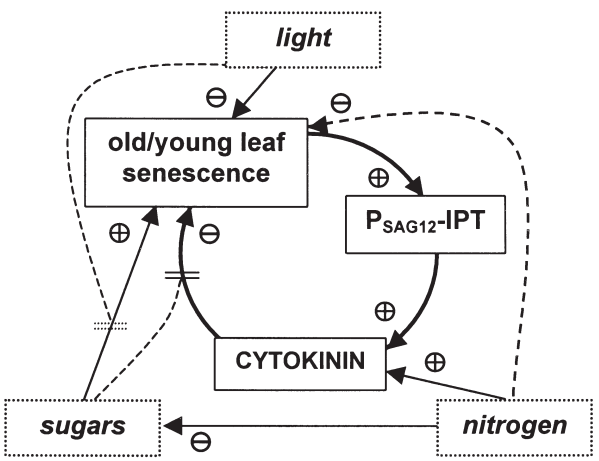

Figure 8. Simplified model of senescence-specific autoregulatory cytokinin biosynthesis, co-regulated by nitrogen, sugars and light. ⊖, Inhibition; ⊕, acceleration; ═, block; ▫▫▫, partial block. This model is modified after Wingler *et al*. (1998), also summarizing information by Gan & Amasino (1997) and results in the present paper. For further explanation, see text.

apical dominance as found in tobacco expressing copper-inducible IPT in the roots, which are the main site of cytokinin biosynthesis in wild-type plants (McKenzie *et al*. 1998). The 6–15-fold increase in the levels of free Z(R) equivalents (and up to 100-fold increase in levels of total ZR equivalents; Table 1) of the oldest SAG–IPT leaves resulted in a chlorophyll content that was 10 times the content in the WT. Furthermore, the chlorophyll content in the oldest leaves of the homozygous SAG–IPT plants was 20% higher than that of the hemizygous SAG–IPT plants, while the levels of ZR equivalents were increased by 40% (free Z) to 100% (free ZR equivalents) relative to the levels in hemizygous plants. These data lead us to conclude that the increased cytokinin levels (ZR equivalents) in the oldest live leaves of hemizygous SAG–IPT are not saturating for delaying senescence. In accordance, young homozygous SAG–IPT leaves, with twice the level of ZR equivalents found in the heterozygote, are less susceptible to loss of chlorophyll, protein and Rubisco at low N supply than the young heterozygous SAG–IPT leaves.

The SAG–IPT plants were engineered to delay leaf senescence by targeting cytokinin biosynthesis to senescing leaves, thus introducing an auto-regulatory 'loop' (Fig. 8). In this paper we demonstrate that the content of Z-type cytokinins is indeed mainly increased in old senescing leaves of the SAG–IPT plants, resulting in a strong delay of visible senescence of the oldest leaves (cf Fig. 8). Analysis of the younger leaves of SAG–IPT plants also demonstrated slightly but significantly elevated ZR equivalents as compared to the WT, indicating that in these plants (i) cytokinins are transported to the younger leaves, or (ii) the promoter is not strictly senescence-specific, or (iii) young leaves increase their cytokinin production in response to the increased sink activity of the older leaves (see below). Some data support the last hypothesis. Firstly, young leaves of tobacco are capable of producing cytokinins (Smart 1994 and references therein). Secondly, no differences in cytokinin levels could be detected in the younger leaves of young WT and SAG–IPT plants supplied with abundant nutrients (data not shown), indicating that the promoter is not activated in young leaves of non-senescing plants. More likely, therefore, promoter activity in the younger leaves of SAG–IPT plants is due to nutrient deficiency-induced senescence enhanced by the high sink activity (for assimilates) of the older leaves of the SAG–IPT plants.

Cytokinin levels and plant N partitioning

Under the present growth conditions, with growth-limiting N supply to induce leaf senescence (Fig. 8), leaf N contents were relatively low, also in the young leaves (< 50% as compared to plants grown with abundant N), with insignificant differences between WT and SAG–IPT in fully mature leaves (results not shown). However, the hemizygous SAG–IPT plants greatly differed from the WT in the distribution of dry matter and N between plant parts (leaves, shoot apex and roots; Fig. 5a,b, respectively). In contrast to WT, SAG–IPT plants distributed more N to the old, senescing leaves at lower layers in the canopy (Fig. 5), associated with a higher cytokinin concentration (Fig. 4). Further, SAG–IPT plants invested less N in the upper layers of the canopy under the present, N-limiting, conditions, even though their cytokinin concentrations were higher than those in WT. As a result, the vertical N profile in the canopy of SAG–IPT plants is inverted as compared to the wild-type profile (Fig. 5b). These effects were even more pronounced in the partitioning of currently absorbed ^{15}N-labelled N (Fig. 6a,b) during the day before the final harvest, suggesting a progressive decline in N accumulation in young leaves of the SAG–IPT plants. This leads to reduced rates of photosynthesis (Fig. 3d; cf Evans 1989) and may eventually lead to early senescence of these young leaves, as indicated by the finding that external application of cytokinins to older leaves results in enhanced senescence of younger, upper leaves (Leopold & Kawase 1964). In SAG–IPT plants, sink activities for N in the various leaf age classes are very similar and more homogeneously distributed than in the WT, although cytokinin levels vary between leaf age classes by at least the same order of magnitude (Fig. 7).

Generally, N distribution between leaf strata within the canopy of plants is closely related to the local light intensity, in a way which suggests optimization of light-use efficiency (Pons *et al*. 1989; Wright & Hammer 1994; Livingston *et al*. 1998). The consequence of the delayed senescence of old leaves and the inverted N profile in the canopy of SAG–IPT plants may be a reduced efficiency of utilization of light and nutrients under field conditions.

The SAG–IPT plants showed reduced N accumulation in young leaves, while retaining N in the oldest leaves which appeared to 'compete' for N with the younger leaves. However, competition for N between senescing and young leaves cannot provide a complete explanation, since N uptake by the roots was also decreased in the SAG–IPT plants (cf Fig. 6a). The reduced N translocation to young and mature leaves in these plants may have various other reasons. Senescing old leaves in the SAG–IPT plants remained strong sinks for N (Fig. 6), and most likely also for C as is often found in response to elevated cytokinin levels (Brenner & Cheikh 1995). Also, respiratory C losses (e.g. for maintenance) increase with increasing N content of leaves (De Visser, Spitters & Bouma 1992). This may result in reduced C availability to the roots of SAG–IPT plants, as indicated by their lower dry weight (Fig. 5a), contributing to a lower root N uptake than in the WT (Fig. 6a). C isotope labelling may resolve this question, by providing information on the sink activity of leaves and roots for C during plant development (cf De Visser *et al*. 1997). Even though the younger leaves of SAG–IPT did not receive as much N as those in the WT, SAG–IPT plants did not increase root N uptake as much as the WT plants, upon supply with (^{15}N-labelled) nitrate. It is not clear whether this apparent suppression of root activity is a direct effect of the raised cytokinin levels and increased sink activity for C and N in the senescing leaves in SAG–IPT plants, or whether it is a more indirect effect, through inhibition of the demand for N ('demand-driven control'; Imsande

& Touraine 1994) of the young leaves. Such a reduced demand may be caused by effects of elevated cytokinin levels on vascular differentiation (Medford *et al*. 1989; Aloni 1995) and/or on callose formation in phloem vessels (Aloni 1995).

In conclusion, we show that the senescence-associated expression of *IPT* in tobacco plants (SAG–IPT) does indeed result in delayed senescence of old leaves (Fig. 8), especially in terms of chlorophyll content, and to a lesser extent in terms of Rubisco level and photosynthesis rate, confirming earlier reports (Wingler *et al*. 1998). In addition, we demonstrate increased endogenous levels of zeatin-type cytokinins in hemi- and homozygous P_{SAG12}–*IPT* plants and report on indirect effects on sink activity of young and old leaves for N and on partitioning of N between plant parts. SAG–IPT plants showed a preferential allocation of N to old, senescing leaves, and a reduced N accumulation in young leaves. This resulted in an inverted vertical N profile within the plant canopy, as compared to the WT.

ACKNOWLEDGEMENTS

The authors thank Wim Valkenburg for nitrogen isotope analysis, and Dr M. van Oijen for valuable comments on the manuscript.

REFERENCES

Aloni R. (1995) The induction of vascular tissues by auxin and cytokinin. In: *Plant Hormones, Physiology, Biochemistry and Molecular Biology* (ed. P.J. Davies), pp. 531–546. Kluwer Academic Publishers, Dordrecht.

Brenner M.L. & Cheikh N. (1995) The role of hormones in photosynthate partitioning and seed filling. In: *Plant Hormones, Physiology, Biochemistry and Molecular Biology* (ed P.J. Davies), pp. 649–670. Kluwer Academic Publishers, Dordrecht.

von Caemmerer S. & Farquhar G.D. (1981) Some relationships between the biochemistry of photosynthesis and gas exchange of leaves. *Planta* **153,** 376–387.

Deléens E., Cliqvet J.B. & Prioul J.L. (1994) Use of ^{13}C and ^{15}N plant label near natural abundance for monitoring carbon and nitrogen partitioning. *Australian Journal of Plant Physiology* **21**, 133–146.

De Visser R., Spitters C.J.T. & Bouma T.J. (1992) Energy cost of protein turnover: theoretical calculation and experimental estimation from regression of respiration on protein concentration of full-grown leaves. In: *Molecular, Biochemical and Physiological Aspects of Plant Respiration* (eds H. Lambers & L.H.W. van der Plas), pp. 493–508. SPB Academic Publishing, The Hague.

De Visser R., Vianden H. & Schnyder H. (1997) Kinetics and relative significance of remobilized and current C and N incorporation in leaf and root growth zones of *Lolium perenne* after defoliation: assessment by ^{13}C and ^{15}N steady-state labelling. *Plant, Cell and Environment* **20,** 37–46.

Evans J.R. (1989) Photosynthesis – the dependence on nitrogen partitioning. In: *Causes and Consequences of Variation in Growth Rate and Productivity of Higher Plants* (eds H. Lambers, M.L. Cambridge, H. Konings & T.L. Pons), pp. 159–174. SPB Academic Publishing, The Hague.

Gan S. & Amasino R.M. (1995) Inhibition of leaf senescence by autoregulated production of cytokinin. *Science* **270,** 1986–1988.

Gan S. & Amasino R.M. (1997) Making sense of senescence. Molecular genetic regulation of leaf senescence. *Plant Physiology* **113,** 313–319.

Goldthwaite J. (1988) Hormones in plant senescence. In: *Plant Hormones and their Role in Plant Growth and Development* (ed. P.J. Davies), pp. 553–573. Kluwer Academic Publishers, Dordrecht.

Grbic V. & Bleecker A.B. (1995) Ethylene regulates the timing of leaf senescence in *Arabidopsis*. *Plant Journal* **8,** 595–602.

Guitman M.R., Arnozis P.A. & Barneix A.J. (1991) Effect of source–sink relations and nitrogen nutrition on senescence and N remobilization in the flag leaf of wheat. *Physiologia Plantarum* **82,** 278–284.

Hikosaka K. & Terashima I. (1995) A model of the acclimation of photosynthesis in the leaves of C_3 plants to sun and shade with respect to nitrogen use. *Plant, Cell and Environment* **18,** 605–618.

Imsande J. & Touraine B. (1994) N demand and the regulation of nitrate uptake. *Plant Physiology* **105,** 3–7.

Inskeep W.P. & Bloom P.R. (1985) Extinction coefficients of chlorophyll a and b in N,N-dimethylformamide and 80% acetone. *Plant Physiology* **77,** 483–485.

John I., Drake R., Farrell A., Cooper W., Lee P., Horton P. & Grierson D. (1995) Delayed leaf senescence in ethylene-deficient ACC-oxidase antisense tomato plants: molecular and physiological analysis. *Plant Journal* **7,** 483–490.

Jordi W., Pot C.S., Stoopen G.M. & Schapendonk A.H.C.M. (1994) Effect of light and gibberellic acid on photosynthesis during leaf senescence of *Alstroemeria* cut flowering stems. *Physiologia Plantarum* **90,** 293–298.

Jordi W., Stoopen G.M., Argiroudi I., in't Veld I., Heinen P. & van Tol H. (1996) Accumulation of a 50-kDa protein during leaf senescence of *Alstroemeria* cut flowering stems. *Physiologia Plantarum* **98,** 819–823.

Leopold A.C. & Kawase Y. (1964) Benzyladenine effects on bean leaf growth and senescence. *American Journal of Botany* **51,** 294–298.

Livingston N.J., Whitehead D., Kelliher F.M., Wang Y.P., Grace J.C., Walcroft A.S., Byers J.N., McSeveny T.M. & Millard P. (1998) Nitrogen allocation and carbon isotope fractionation in relation to intercepted radiation and position in a young *Pinus radiata* D. Don tree. *Plant, Cell and Environment* **21,** 795–803.

McKenzie M.J., Mett V., Reynolds P.H.S. & Jameson P.E. (1998) Controlled cytokinin production in transgenic tobacco using a copper-inducible promoter. *Plant Physiology* **116,** 969–977.

Medford J.L., Horgan R., El-Sawi Z. & Klee H.J. (1989) Alteration of endogenous cytokinins in transgenic plants using chimeric isopentenyl transferase gene. *Plant Cell* **1,** 403–413.

Niyogi K.K. (1999) Photoprotection revisited: genetic and molecular approaches. *Annual Review of Plant Physiology and Plant Molecular Biology* **50,** 333–359.

Pons T.L., Schieving F., Hirose T. & Werger M.J.A. (1989) Optimization of leaf nitrogen allocation for canopy photosynthesis in *Lysimachia vulgaris*. In: *Causes and Consequences of Variation in Growth Rate and Productivity in Higher Plants* (eds H. Lambers, M.L. Cambridge, H. Konings & T.L. Pons), pp. 175–186. SPB Academic Publishing, The Hague.

Redig P., Motyka V., van Onckelen H.A. & Kaminek M. (1997) Regulation of cytokinin oxidase activity in tobacco callus expressing the T-DNA ipt gene. *Physiologia Plantarum* **99,** 89–96.

van Rhijn J.A., Heskamp H.H., Davelaar E., Jordi W., Leloux M.S. & Brinkman U.A.Th. (2000) Quantitative analysis of glycosylated and aglycon cytokinins at sub-picomol level by micro-LC and capillary-LC combined with electrospray tandem mass spectrometry. *Journal of Chromatography A* in press.

Schapendonk A.H.C.M., Spitters C.J.T. & de Vos A.L.F. (1990) Comparison of nitrogen utilization of diploid and tetraploid perennial ryegrass genotypes using a hydroponic system. In: *Genetic Aspects of Plant Mineral Nutrition* (eds N. El Bassam, M. Dambroth & B.C. Loughman), pp. 299–306. Kluwer Academic Publishers, Dordrecht.

Schmülling T., Schäfer S. & Romanov G. (1997) Cytokinins as regulators of gene expression. *Physiologia Plantarum* **100,** 505–519.

Schnyder H. & De Visser R. (1999). Fluxes of reserve-derived and currently assimilated carbon and nitrogen in perennial ryegrass recovering from defoliation. The regrowing tiller and its component functionally distinct zones. *Plant Physiology* **119,** 1423–1435.

Smart C.M. (1994) Tansley Review No. 64: Gene expression during leaf senescence. *New Phytologist* **126,** 419–448.

Smart C.M., Scofield S.R., Bevan M.W. & Dyer T.A. (1991) Delayed leaf senescence in tobacco plants transformed with tmr, a gene for cytokinin production in *Agrobacterium*. *The Plant Cell* **3**, 647–656.

Steiner A.A. (1984) The universal nutrient solution. In: *Proceedings of the Sixth International Congress on Soilless Culture*, Lunteren. pp. 633–650. International Society for Soilless Culture, Wageningen.

Thimann K.V. (1980) The senescence of leaves. In: *Senescence in Plants* (ed. K.V. Thimann), pp. 86–115. CRC Press, Boca Raton.

Vonk C.R., Davelaar E. & Ribôt S.A. (1986) The role of cytokinins in relation to flower-bud blasting in *Iris* cv. Ideal: cytokinin determination by an improved enzyme-linked immunosorbent assay. *Plant Growth Regulation* **4,** 65–74.

Wang J., Letham D.S., Cornish E. & Stevenson K.R. (1997) Studies of cytokinin action and metabolism using tobacco plants expressing either the ipt or the GUS gene controlled by a chalcone synthase promoter. II. Ipt and GUS gene expression, cytokinin levels and metabolism. *Australian Journal of Plant Physiology* **24,** 673–683.

Wingler A., von Schaewen A., Leegood R.C., Lea P.J. & Quick W.P. (1998) Regulation of leaf senescence by cytokinin, sugars, and light. Effects on NADH-dependent hydroxypyruvate reductase. *Plant Physiology* **116,** 329–335.

Wright G.C. & Hammer G.L. (1994) Distribution of nitrogen and radiation use efficiency in peanut canopies. *Australian Journal of Agricultural Research* **45,** 565–574.

Zhang R., Zhang X., Wang J., Letham D.S., McKinney S.A. & Higgins T.J.V. (1995) The effect of auxin on cytokinin levels and metabolism in transgenic tobacco tissue expressing an ipt gene. *Planta* **196,** 84–94.

Received 18 July 1999; received in revised form 18 October 1999; accepted for publication 18 October 1999